

## Chaos and coherence in coupled lasers

K. S. Thornburg, Jr., M. Möller,\* and Rajarshi Roy  
*School of Physics, Georgia Institute of Technology, Atlanta, Georgia 30332*

T. W. Carr,† R.-D. Li,‡ and T. Erneux  
*Université Libre de Bruxelles, Optique Nonlinéaire Théorique, Campus Plaine, C.P. 231, 1050 Bruxelles, Belgium*  
 (Received 5 August 1996)

A fundamental chaotic instability in a system of two coupled lasers is investigated both experimentally and theoretically. The amplitude instability and mutual coherence of the light emitted by the lasers is investigated as a function of the detuning and coupling parameters. A quantitative comparison of the intensity fluctuations is made with numerical simulations that include noise in the laser detuning. [S1063-651X(97)03904-4]

PACS number(s): 05.45.+b, 42.50.Lc, 42.55.Rz

Haken's seminal analogy between fluid dynamics and laser instabilities initiated extensive studies of the Lorenz-like chaotic dynamics of the single mode far-infrared ammonia laser over the last two decades [1,2]. While this is conceptually the simplest chaotic laser system, it is also of great fundamental interest that two single-mode lasers that are stable individually can exhibit a chaotic instability when coupled [3,4]. Such a system provides a beautiful illustration of the rich and complex dynamical behavior of two coupled nonlinear oscillators. Pairs of neurons [5], pacemaker cells [6], chemical oscillators [7], and Josephson junctions [8] provide other examples of coupled nonlinear oscillator systems. It has been theoretically recognized that the amplitudes of the coupled oscillators can display a rich variety of unstable behaviors for certain regimes of coupling strength [9]. However, there are no experiments on physical systems that have quantitatively probed the relationship between the chaotic amplitude instability and phase coherence of coupled nonlinear oscillators. In this paper we report the results of precise measurements of the amplitude dynamics and phase coherence of coupled lasers and make quantitative comparisons with numerical models.

Many studies of coupled lasers have been motivated by the need for high power coherent sources. Coupled semiconductor, solid state, and CO<sub>2</sub> lasers have been studied [4,10–12], but it is the spatial properties of the output radiation that have received the most attention, rather than the dynamical characteristics of the emitted light [13]. Here, we study the chaotic dynamics and mutual coherence [14] of two coupled single-mode Nd:YAG (neodymium doped yttrium aluminum garnet) lasers that are detuned from each other by a very small amount (roughly 1 part in 10<sup>8</sup> of the oscillator frequency) and for which we can vary the coupling strength over many orders of magnitude.

The following equations describe the time evolution of the complex, slowly varying electric field  $E$  and gain  $G$  of a pair of spatially coupled, single transverse and longitudinal mode class B lasers [15,16]

$$\frac{dE_1}{dt} = \tau_c^{-1}[(G_1 - \alpha)E_1 - \kappa E_2] + i\omega_1 E_1, \quad (1a)$$

$$\frac{dG_1}{dt} = \tau_f^{-1}(p_1 - G_1 - G_1|E_1|^2), \quad (1b)$$

$$\frac{dE_2}{dt} = \tau_c^{-1}[(G_2 - \alpha_2)E_2 - \kappa E_1] + i\omega_2 E_2, \quad (1c)$$

$$\frac{dG_2}{dt} = \tau_f^{-1}(p_2 - G_2 - G_2|E_2|^2). \quad (1d)$$

In these equations,  $\tau_c$  is the cavity round trip time ( $\approx 450$  ps for a cavity of length of 6 cm),  $\tau_f$  is the fluorescence time of the upper lasing level of the Nd<sup>3+</sup> ion (240  $\mu$ s for the 1064 nm transition),  $p_1$  and  $p_2$  are the pump coefficients,  $\alpha_1$  and  $\alpha_2$  are the cavity loss coefficients, and  $\omega_1$  and  $\omega_2$  (angular frequencies) are the detunings of the lasers from a common cavity mode, respectively. The lasers are coupled linearly to each other with strength  $\kappa$ , assumed to be small, and the sign of the coupling terms is chosen to account for the observed stable phase-locked state in which the lasers have a phase difference of 180°. For laser beams of Gaussian intensity profile and  $1/e^2$  beam radius  $r$  the coupling strength, as determined from the overlap integral of the two fields, is defined as  $\kappa = \exp(-d^2/2r^2)$ . Control parameters are the frequency detuning of the lasers ( $\Delta\omega = \omega_2 - \omega_1$ ) and the coupling coefficient  $\kappa$ .

The dependence of the system dynamics on parameters can be numerically investigated by integrating Eqs. (1) using different values of  $\kappa$  and  $\Delta\omega$ . Figure 1 displays the predicted amplitude instability of the two lasers and its relationship to the coherence of the laser light as a function of both the laser separation  $d$  and the detuning  $\Delta\omega$ . The height of the graph shows the largest intensity value of laser 1 recorded during the 5 ms integration time. The color coding shows the degree of mutual coherence between the two lasers, as measured by

\*Permanent address: Westfälische Wilhelms-Universität, Institut für Angewandte Physik, Corrensstrasse 2/4, 48149 Münster, Germany.

†Present address: Naval Research Lab, Code 6700. 3, Special Project in Nonlinear Science, Washington, D.C. 20375-5000.

‡Present address: HGM Medical Lasers Inc., 3959 West 1820 South, Salt Lake City, UT 84104.

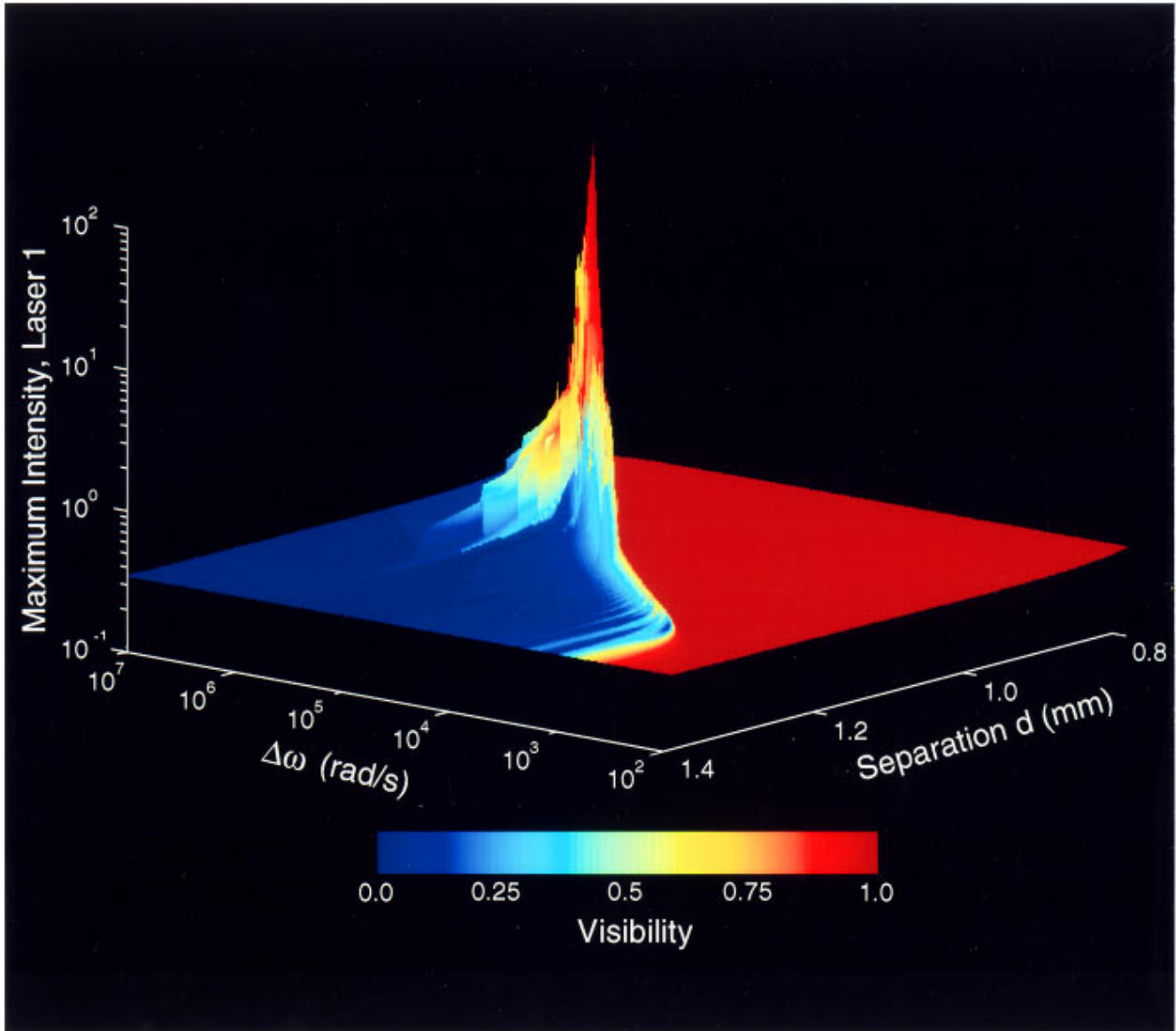


FIG. 1. (Color). Numerically computed parameter space plot of the amplitude instability of two lasers as a function of both the separation  $d$  and detuning  $\Delta\omega$ . Here  $p_1=0.053$ ,  $p_2=0.051$ ,  $\alpha_1=\alpha_2=0.04$ , and  $r=225\ \mu\text{m}$ . We use pump parameters that differ by a few percent in the simulation to account for the fact that the two lasers may be nonidentical in the experiment. The height of the graph indicates the largest intensity value recorded at a given value of separation and detuning, while the color of the graph denotes the degree of mutual coherence between the two lasers, as indicated by the fringe visibility. Blue colors indicate low visibilities, while red colors indicate visibilities approaching unity, as shown in the legend.

the fringe visibility. The visibility  $V$  of the fringe pattern formed by the small angle interference of the laser beams is defined as  $V=(I_{\max}-I_{\min})/(I_{\max}+I_{\min})$  where  $I_{\max}$  and  $I_{\min}$  are adjacent maxima and minima in the fringe profile. The fringe visibility is directly proportional to the absolute value of the complex degree of mutual coherence [14]. Low visibilities, shown as blue colors in this figure, indicate states of low mutual coherence, while reds indicate visibilities approaching one and therefore high degrees of mutual coherence. One can clearly see from Fig. 1 that the area where the intensity instabilities exist occurs just before the onset of phase locking and that significant intensity oscillations appear only around a rather narrow band of detuning values between  $10^5$  and  $10^6\ \text{s}^{-1}$ . A single positive Lyapunov exponent was computed in this regime with a typical value of

$\approx 10^4\ \text{s}^{-1}$ , demonstrating the chaotic nature of the instability.

Insight into the amplitude instability can be obtained by considering the special case of identical laser parameters and by assuming that the two laser amplitudes and gains are identical. Equations (1) then reduce to

$$\frac{d\mathcal{E}}{dt} = \tau_c^{-1}[G - \alpha - \kappa \cos(\Phi)]\mathcal{E}, \quad (2a)$$

$$\frac{dG}{dt} = \tau_f^{-1}(p - G - G\mathcal{E}^2), \quad (2b)$$

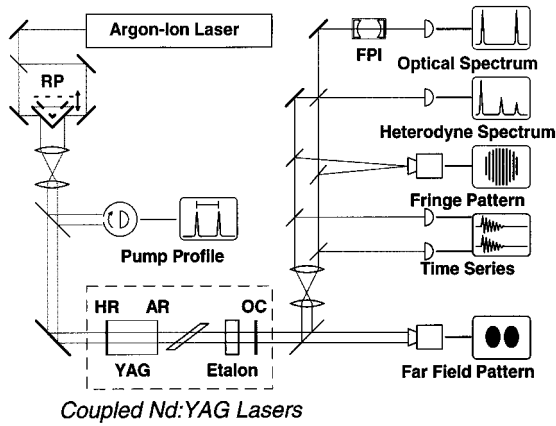


FIG. 2. Experimental system for generating two laterally coupled lasers in a Nd:YAG crystal and observing the amplitude instability. RP is a rectangular prism; translating this device changes the pump beam separation, and thus the infrared beam separation. The Nd:YAG crystal is coated for high reflectivity (HR) on one side and antireflection coated (AR) on the other. The output coupler (OC) is 2% transmissive; both mirrors at flat. FPI is a scanning Fabry-Pérot interferometer, and as used to measure the mode spectrum of both lasers.

$$\frac{d\Phi}{dt} = 2\tau_c^{-1}\kappa \sin(\Phi) + \Delta\omega \quad (2c)$$

for the laser amplitudes  $|E_1| = |E_2| = \mathcal{E}$ , gains  $G_1 = G_2 = G$  and phase difference  $\Phi = \phi_2 - \phi_1$ , where  $\phi_1$  is the phase of the field  $E_i$ .

Equations (2a)–(2c) are the rate equations describing a single mode class B laser with variable losses. The phase equation can be integrated exactly, and  $\Phi(t)$  is an unbounded function of time if the detuning  $|\Delta\omega|$  exceeds a critical detuning  $\Delta\omega_c$ , where

$$\Delta\omega_c \equiv 2\kappa\tau_c^{-1}. \quad (3)$$

This is the critical condition for an amplitude instability [4]; we also note that the lasers are phase locked for detunings smaller than  $\Delta\omega_c$  [16]. If condition (3) is obeyed, then the laser equations (2a) and (2b) are periodically modulated by the  $\cos[\Phi(t)]$  term. The frequency of these modulations is given by

$$\omega_M \equiv \sqrt{\Delta\omega^2 - \Delta\omega_c^2}. \quad (4)$$

On the other hand, it is known that the laser relaxation oscillation frequency  $\omega_R$  ( $= 2\pi\nu_R$ ) for small  $\tau_c/\tau_f$  and  $\kappa=0$  is given by

$$\omega_R \equiv \left( \frac{2(p-\alpha)}{\tau_c\tau_f} \right)^{1/2}. \quad (5)$$

This implies the possibility of subharmonic resonance if the ratio of  $\omega_M$  to  $\omega_R$  is close to an integer. These resonances then produce branches of subharmonic solutions which explain the destabilization of the laser system [17,18].

We have tested the prediction of the amplitude instability with the experimental system of Fig. 2, which consists of two parallel, laterally separated lasers created by pumping a

single Nd:YAG rod of 5 mm length and diameter in a plane parallel cavity. The pump beams are generated from the argon ion laser output ( $\lambda = 514.5$  nm) by a system of beam splitters and prisms that ensure parallel propagation at an adjustable separation symmetric with respect to the YAG rod axis. The optical cavity consists of one high reflection coated end face of the rod and of an external planar output coupler with 2% transmittance. A Brewster plate and thick etalon within the cavity ensure linear polarization and single longitudinal mode operation. The lasers were operated at approximately 33% above threshold pump power. For these parameters, the relaxation oscillation frequency,  $\nu_R$ , is of the order of 100 kHz. The frequency detuning between the two lasers can be adjusted by tilting the output coupler slightly, thereby introducing a minute difference in cavity lengths.

Thermal lensing induced in the YAG crystal by the pump beams of waist radius  $\approx 20$   $\mu\text{m}$  is responsible for generating two stable, separate cavities [16]. The TEM<sub>00</sub> infrared laser beams have radii (at  $1/e^2$  of the maximum intensity of the Gaussian profile) of  $r \approx 200$   $\mu\text{m}$  and their overlap may be continuously changed by varying the lateral separation  $d$  of the pump beams over a range of 0.5 mm–3 mm. The pump beam separation and profiles are measured directly by a rotating slit technique. In this range, there is no appreciable overlap of the pump beams and coupling is entirely due to the spatial overlap of the infrared laser fields.

The individual output intensity time series are recorded with fast photodetectors and a two channel digital oscilloscope. The optical frequency difference of the lasers is measured with a radio frequency spectrum analyzer after combining the two beams on a photodetector. A scanning Fabry-Pérot interferometer was used to ensure that both lasers oscillated only on a single longitudinal mode.

The change of dynamical behavior of the detuned, coupled system can be seen as the separation of the pump beams is varied. For a large separation ( $d \geq 1.20$  mm) the lasers were stable and incoherent. The visibility of the fringes was low ( $V \approx 0$ ), and the heterodyne signal was measured to be between 30 and 40 MHz. For a small separation ( $d \leq 0.8$  mm), the lasers are stable and phase locked. The fringe visibility was high ( $V \approx 1$ ), and the heterodyne signal was absent since the lasers were frequency locked. Figure 3(a) shows a typical intensity time trace characteristic of the unstable regime. Large bursts of the intensity occur, separated by quiescent periods. Here the lasers were separated by 1.03 mm, which implies  $\kappa \approx 2.0 \times 10^{-5}$ . Using Eq. (3), we find that the condition for an amplitude instability requires  $|\Delta\omega| > 10^5$   $\text{s}^{-1}$ , which is verified in our experiments ( $\Delta\omega \approx 1$  MHz). The intermediate visibility of  $V = 0.20$  signifies the onset of phase locking. The experimentally measured visibilities are in excellent agreement with the numerically computed values represented in Fig. 1.

In the experiment, a substantial amount of fluctuation in the detuning between the two lasers was observed; the beat signal frequency in the unstable regime fluctuated between 0 and 10 MHz. In order to obtain quantitative comparison between measured intensity time series and simulations, we numerically investigated the behavior of Eqs. (1) with a stochastic detuning term, such that  $\Delta\omega(t) = \omega_2 - \omega_1$ , where  $\omega_i = \omega_{0,i} + \delta\omega_i(t)$ . Here  $\delta\omega_i(t)$  is a colored noise term of

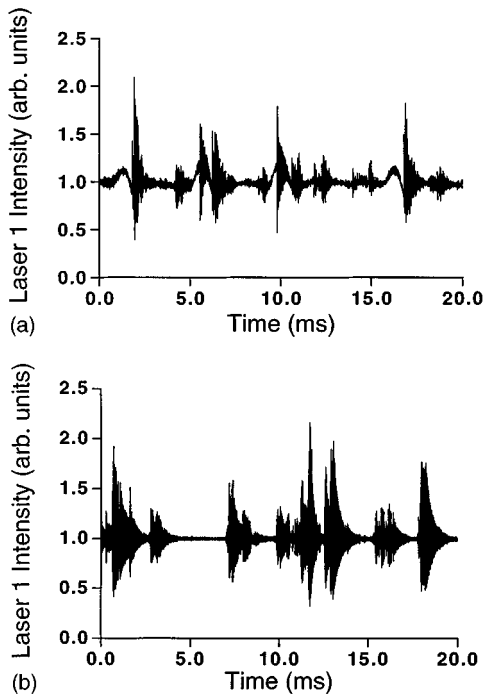


FIG. 3. Intensity time traces of (a) experiment and (b) numerical simulation. The time trace in (a) was measured at a pump separation of  $d = 1.03$  mm, and illustrates the bursting nature of the amplitude instability. The average interspike interval (ISI) is 1.9 ms, the normalized standard deviation  $\sigma_I/\bar{I} = 0.10$ , and the standard deviation of the detuning  $\sigma_{\Delta\omega} \approx 10^6$  s $^{-1}$ . (b) The numerically computed time trace of the intensity of laser 1 with an exponentially correlated, stochastic detuning term of strength  $D = 5 \times 10^9$  s $^{-1}$  and correlation time  $\lambda^{-1} = 3$  ms. The mean detuning  $\Delta\omega_0 = 5 \times 10^5$  s $^{-1}$ , and the standard deviation of the detuning  $\sigma_{\Delta\omega} = 1.4 \times 10^6$  s $^{-1}$ . The average ISI was 1.7 ms, and  $\sigma_I/\bar{I} = 0.12$ . The cavity losses were taken to be 4% and the lasers were pumped one-third above threshold, with a 0.5% asymmetry.

strength  $D$  and correlation time  $\lambda^{-1}$ , with the properties  $\langle \delta\omega_i(t) \rangle = 0$  and  $\langle \delta\omega_i(t) \delta\omega_j(t + \Delta t) \rangle = \delta_{ij} D \lambda \exp(-\lambda |\Delta t|)$  [19].

We used three different statistical measures to compare the numerically simulated and experimental traces—the normalized standard deviation of the intensity  $\sigma_I/\bar{I}$ , the average interspike interval (ISI), and the standard deviation of the detuning  $\sigma_{\Delta\omega}$ . The average ISI is determined by measuring

the average time between adjacent bursts whose intensities are greater than some threshold, here defined to be 1.2 times the average intensity. To avoid counting the same burst twice, a “quiescence time”  $\tau_q$  of 0.8 ms was used such that a new spike would be detected no sooner than  $\tau_q$ . The standard deviation of the detuning in the experiments was measured to be on the order of 10 MHz or less; numerically,  $\sigma_{\Delta\omega} = \sqrt{D\lambda}$ . Using these statistical measures, the parameters  $D$  and  $\lambda$  were adjusted to give quantitative agreement between the observed experimental results and the numerical simulations. The range of parameters  $D$  and  $\lambda$  that gave quantitative agreement with experiment is very limited;  $D \sim O(10^9$  s $^{-1})$  and  $\lambda^{-1} \sim O(10^{-3}$  s). Figure 3(b) shows a good match with the experimental data.

In conclusion, we have demonstrated a fundamental amplitude instability of two coupled lasers and its relationship to the mutual coherence of the total field. Theoretical and numerical predictions, using a dynamical model, of the range of coupling strengths where the instability is expected to occur agree very well with experimental observations. For large separations, both the model and experiment reveal stable intensities and no appreciable coherence. As the separation is decreased to just above the phase-locking point, large amplitude fluctuations are observed, in agreement with numerical predictions. The laser fields exhibit a low degree of mutual coherence for this range of coupling strength. It was necessary to include stochastic detuning fluctuations to achieve quantitative agreement between experimental and simulation in the unstable regime. Finally, for even smaller separations, phase locking is achieved. The lasers are now found to be stable, mutually coherent, and frequency locked. These studies are directly relevant to the design of laser arrays; they also reveal a rich and complex dynamical scenario which should be systematically explored in the future for a variety of different oscillator systems.

We acknowledge support from the Division of Chemical Sciences, Office of Basic Energy Sciences, Office of Energy Research, U.S. Department of Energy, and the Office of Naval Research. M.M. acknowledges support from the Deutsche Forschungsgemeinschaft (DFG, Germany). R.R. thanks Neal Abraham, Edgar Knobloch, and Steve Strogatz for helpful discussions. T.E. acknowledges support from U.S. Air Force Office of Scientific Research Grant AFOSR-93-1-0084, National Science Foundation Grant DMS-9308009, the Fonds National de la Recherche Scientifique (Belgium), and the InterUniversity Attraction Pole of the Belgian government.

[1] H. Haken, *Phys. Lett. A* **53**, 77 (1975).

[2] C. O. Weiss and R. Vilaseca, *Dynamics of Lasers* (VCH, Weinheim, 1991); A. C. Newell and J. V. Moloney, *Nonlinear Optics* (Addison-Wesley, New York, 1992).

[3] S. S. Wang and H. G. Winful, *Appl. Phys. Lett.* **52**, 1774 (1988); H. G. Winful and S. S. Wang, *ibid.* **53**, 1894 (1988).

[4] A. V. Bondarenko, A. F. Glova, S. N. Kozlov, F. V. Lebedev, V. V. Likhanskii, A. P. Napartovich, V. D. Pis'mennyi, and V. P. Yartsev, *Zh. Eksp. Teor. Fiz.* **95**, 807 (1989) [*Sov. Phys. JETP* **68**, 461 (1989)].

[5] M. Kawato and R. Suzuki, *J. Theor. Biol.* **86**, 547 (1980).

[6] A. Winfree, *The Geometry of Biological Time* (Springer-Verlag, Berlin, 1990).

[7] K. Bar-Eli, *Physica D* **14**, 242 (1985).

[8] S. Watanabe, S. H. Strogatz, H. S. J. van der Zant, and T. P. Orlando, *Phys. Rev. Lett.* **75**, 45 (1995).

[9] D. G. Aronson, G. B. Ermentrout, and N. Kopell, *Physica D* **41**, 403 (1990).

[10] V. V. Likhanskii and A. P. Napartovich, *Usp. Fiz. Nauk* **160**, 101 (1990) [*Sov. Phys. Usp.* **33**, 228 (1990)]; B. Ozygus and

- H. Laabs, *Chaos, Solitons Fractals* **4**, 1559 (1994).
- [11] *Diode Laser Arrays*, edited by D. Botez and D. R. Scifres (Cambridge University Press, Cambridge, England, 1994).
- [12] *High-Power Multibeam Lasers and Their Phase Locking*, edited by F. V. Lebedev and A. P. Napartovich, Proc. SPIE Vol. 2109 (SPIE, Bellingham, WA, 1993).
- [13] H. Winful and R. K. DeFreez, in *Diode Laser Arrays* (Ref. [11]).
- [14] L. Mandel and E. Wolf, *Optical Coherence and Quantum Optics* (Cambridge University Press, New York, 1995), p. 163.
- [15] F. T. Arecchi, G. L. Lippi, G. P. Puccioni, and J. R. Tredicce, *Opt. Commun.* **51**, 308 (1994).
- [16] L. Fabiny, P. Colet, Rajarshi Roy, and D. Lenstra, *Phys. Rev. A* **47**, 4287 (1993).
- [17] T. Erneux, S. M. Baer, and P. Mandel, *Phys. Rev. A* **35**, 1165 (1987).
- [18] I. B. Schwartz, *Phys. Lett. A* **126**, 411 (1988).
- [19] R. F. Fox, I. R. Gatland, R. Roy, and Gautam Vemuri, *Phys. Rev. A* **38**, 5938 (1988); R.L. Honeycutt, Ph.D. thesis, Georgia Institute of Technology, 1990.